Molecular Cancer Therapeutics

# Protein Kinase Inhibitor H89 Enhances the Activity of *Pseudomonas* Exotoxin A–Based Immunotoxins

Xiufen Liu[1], Fabian Müller[1], Alan S. Wayne[2], and Ira Pastan[1]

## Abstract

HA22 (Moxetumomab pasudotox) is a recombinant immunotoxin (RIT), composed of an anti-CD22 Fv fused to a truncated portion of *Pseudomonas* exotoxin A. HA22 is in clinical trials to treat patients with hairy cell leukemia and acute lymphoblastic leukemia (ALL). LMB-11 is an improved variant of HA22 with reduced immunogenicity, has a longer half-life in the blood and high activity *in vitro* and in a Burkitt lymphoma model *in vivo*. Searching for RIT enhancing combination therapies, we found the protein kinase A inhibitor H89 to enhance LMB-11 and HA22 activity 5- to 10-fold on ALL cell lines and on patient-derived ALL samples. In addition, H89 increased the activity of mesothelin-targeting RITs SS1P (38-fold) and RG7787 (7-fold) against the cervical cancer cell line KB31. Unexpectedly we found that the enhancement by H89 was not because of inhibition of protein kinase A; it was partially recapitulated by inhibition of S6K1, which led to inactivation of its downstream targets rpS6 and GSK3β, resulting in a fall in MCL1 levels. H89 increased the rate of ADP-ribosylation of eukaryotic elongation factor 2, enhancing the arrest of protein synthesis and the reduction of MCL1 in synergy with the RIT. In summary, H89 increased RIT activity by enhancing the two key events: ADP-ribosylation of eEF2 and reduction of MCL1 levels. Significant enhancement was seen with both CD22- and mesothelin-targeting RITs, indicating that H89 might be a potent addition to RIT treatment of CD22-positive ALL and mesothelin-expressing solid tumors. *Mol Cancer Ther; 15(5); 1053–62. ©2016 AACR.*



## Introduction

Acute lymphoblastic leukemia (ALL) is the most common childhood cancer (1). Current treatment regimens result in 80% long-term survival (2); however, disease relapse is associated with a poor outcome (3) and ALL remains the leading cause of cancer-related deaths in children and young adults (2, 4). To further improve response rates, novel treatment options have been developed which are currently in clinical evaluation (5–10).

As part of the effort to find new ALL therapeutics, we generated *Pseudomonas* exotoxin A (PE)–derived recombinant immunotoxins (RIT). To do this, the binding domain of the toxin is replaced with an $F_V$ portion of a monoclonal antibody, which is chosen to target cancer cells, but not normal essential tissues (11, 12). For targeting B-ALL and other B-cell malignancies, CD22 is a favorable target molecule (13, 14). HA22 (also known as CAT-8015 or Moxetumomab pasudotox; ref.15) is a CD22-targeting RIT in which an anti-CD22 $F_V$ is fused to a 38 kDa fragment of PE. HA22 produced complete remissions in nearly 50% of patients with drug-resistant HCL (15) and in 24% of children with chemotherapy-refractory ALL (5, 16). In attempt to improve the activity of CD22-targeting RITs, we developed LMB-11 in which the $F_v$ was replaced with an $F_{ab}$, and immunogenicity was reduced by deleting most of domain II and modifying seven B-cell epitopes in domain III (17). LMB-11 is more active than HA22 in a CA46 Burkitt lymphoma animal model, where it produced complete regressions of tumors (18).

The mechanism by which RITs kill cells is complex and not completely understood. After binding to the surface receptor and internalization, RITs are cleaved by furin and traverse cells through various endocytic compartments using retrograde trafficking to reach the endoplasmic reticulum and ultimately the cytosol. There, PE catalyzes ADP ribosylation of eukaryotic elongation factor 2 (eEF2), which arrests protein synthesis and leads to apoptosis (5, 12, 19).

Protein kinases play an essential role in all aspects of signal transduction pathways involving cell growth, proliferation, metabolism, and disease. Similarly, protein kinases also modulate how effectively RITs traverse the various cellular compartments. We showed that small GTPases ARF1 and ARF4 are involved in the regulation of RIT trafficking (20) and have identified the insulin receptor (21) and the Src-family kinase HCK (22) as important modulators of the activity of HA22 as well as the mesothelin-targeting RIT SS1P. Protein kinase A (PKA) has been implicated in numerous cellular processes. The study of PKA function has been dominated by the use of pharmacological inhibitors. One of these, H89, is a strong PKA inhibitor with the ability to readily cross the cell membrane, with preclinical activity demonstrated *in vitro* and *in vivo* (23–26).

Here, we show that H89 strongly enhances the activity of the CD22 targeting RITs LMB-11 and HA22 on ALL cell lines and patient-derived ALL cells and of a mesothelin-targeting RIT on a

[1]Laboratory of Molecular Biology, Center for Cancer Research, National Cancer Institute, National Institutes of Health, Bethesda, Maryland. [2]Division of Hematology, Oncology and Blood and Marrow Transplantation, Children's Center for Cancer and Blood Diseases, Children's Hospital Los Angeles, Norris Comprehensive Cancer Center, Keck School of Medicine, University of Southern California, Los Angeles, California.

**Note:** Supplementary data for this article are available at Molecular Cancer Therapeutics Online (http://mct.aacrjournals.org/).

X. Liu and F. Müller contributed equally to this article.

**Corresponding Author:** Ira Pastan, National Cancer Institute National Institutes of Health, 37 Convent Dr, Rm 5106, Bethesda, MD 20892-4264. Phone: 301-496-4797; Fax: 301-402-1344; E-mail: pastani@mail.nih.gov

**doi:** 10.1158/1535-7163.MCT-15-0828

cervical cancer cell line. The strong enhancement is because of more efficient ADP ribosylation of eEF2 by RIT in combination with a synergistic reduction of MCL1 by the two drugs in combination.

## Materials and Methods

### Reagents

HA22 (27), LMB-11 (18), LMB-31, and SS1P (28, 29) were purified as described (30). Immunotoxin LMB-31, an inactive form of LMB-11, was generated by site-directed mutagenesis changing E553 to D553 in the PE fragment. RG7787 [huSS1 (Fab)-LR-GGS-LO10-PE24] was supplied by Roche Innovation Center, Penzberg, Germany, under a Cooperative Research and Development Agreement (31).

Antibodies detecting p-S6K1(T389), S6K1, p-CREB(S133)/ATF-1, p-rpS6(S240/244), rpS6, p-GSK3β(S9), GSK3β, Bcl2, PARP, cleaved caspase 3, Bax, Bcl-xL, and MCL1 were purchased from Cell Signaling; H89 from Selleck; 8-Br-cAMP, Dibutyl-cAMP, and anti-β-tubulin from Sigma; anti-actin from Abcam; and inhibitors PKI-myristoylated (14–22) amide and S6K1 inhibitor PF4708671 from Tocris Sciences.

### Cell lines

Human ALL cell lines HAL-01, KOPN-8, REH, SEM, NALM-6, and cervical cancer cell line KB31 were cultured in RPMI and supplemented with 10% fetal bovine serum and 1% penicillin–streptomycin at 37°C. The cell lines HAL-01 (32), NALM-6 (9), and KB31 (21) cells were described previously. KOPN-8 and SEM cells were purchased from DSMZ; REH was obtained from ATCC. All the cell lines identities were confirmed by short tandem repeat analysis at the Frederick National Laboratory for Cancer Research in 2012 or 2013. The cells were then frozen in aliquots and thawed as needed.

### WST8 assay

Cytotoxic activity of RITs in combination with inhibitors was determined by growth inhibition assays as described (18). Briefly, 10,000 ALL cells or 5,000 KB31 cells were plated per well in a 96-well format. Treatment was added to the wells 5 hours after plating. Inhibitor or vehicle was added first for 1 hour or as indicated, followed by RIT or 100 μg/mL cycloheximid for positive control. After 72 hours of incubation, WST8 was added. Resulting $OD_{450}$ values were normalized to cycloheximid and medium control.

### Western blot analysis

Cells were washed in phosphate-buffered saline (PBS) and lysed for 30 minutes on ice in modified RIPA buffer (50 mmol/L Tris HCl, 150 mmol/L NaCl, 5 mmol/L EDTA, 1% NP40, 5 μg/mL leupeptin, 5 μg/mL aprotinin, 10 μmol/L PMSF). After high-speed centrifugation, supernatants were analyzed by SDS-PAGE, transferred to PVDF membranes, and subjected to Western blot analysis.

### Internalization and FACS analysis

Internalization of LMB-11 was measured as described (33). Briefly, KOPN-8 cells were treated with or without 10 μmol/L H89 for 1 hour in 6-well plates, 1 μg/mL of LMB-11-Alexa647 was added, and cells were incubated at 37°C for the indicated times. Cells were washed with PBS and stripped 10 minutes with 0.2 M Glycine-HCl (pH 2.5) to remove surface bound LMB-11, washed with FACS buffer (PBS with 5% FBS, 0.1% $NaN_3$), and analyzed by flow cytometry using a FACS Calibur (Becton Dickinson).

### Furin-cleavage assay

The rate of furin cleavage was determined as described (21). KOPN-8 cells were treated with 10 μmol/L H89 or vehicle for 1 hour. One μg/mL of HA22 was added and cells incubated on ice for 30 minutes to saturate HA22 binding. Cells were washed, medium changed, and incubated at 37°C for the indicated times before cell lysis and Western blot analysis.

### ADP ribosylation of eEF2

Cells were lysed in modified RIPA buffer; 5 μg protein from the cell lysates was incubated with 50 ng LMB-11 in ADP-ribosylation buffer [20 mmol/L Tris-HCl (pH 7.4), 1 mmol/L EDTA, 50 mmol/L DTT] with 0.3 μmol/L of 6-biotin-17-NAD (Trevigen) for 60 min at 25°C. Samples were subjected to SDS-PAGE, followed by Western blotting with HRP-conjugated streptavidin to detect biotin-ADP-ribose-eEF2.

### Leucine incorporation assay

Protein synthesis inhibition was performed using a $^3$H-leucine incorporation assay as described (30). A total of 5,000 KOPN-8 cells were plated per well of a 96-well plate with 10 μmol/L H89 or vehicle and treated with various concentrations of LMB-11. After 16 hours, wells were pulsed with 2 μCi $^3$H-Leucine for 2 hours at 37°C. Plates were harvested for readout using a liquid scintillation counter (Wallac).

### FACS analysis of apoptotic cells

KOPN-8 cells in six-well plates were treated with LMB-11 in combination with 10 μmol/L H89 or vehicle for indicated times. Cells were harvested and stained with Annexin V-PE and 7-AAD according to kit instructions (BD Biosciences). Cells were run on a FACS Calibur and data analyzed in FlowJo (TreeStar Inc.).

### Patient samples

Primary ALL blast samples were collected from four patients with CD22-positive pre-B-ALL under protocols approved by the NCI Institutional Review Board. Samples that had been viably cryopreserved and stored in liquid nitrogen were thawed, washed, resuspended in PBS, and injected intravenously in immunodeficient (NSG) mice. Mice were euthanized at disease progression, and whole spleen and bone marrow extracted (spine, hip, and femur by crushing with mortar and pestle). Cells were analyzed by flow for hu-CD19, hu-CD22, and hu-CD10, and viably frozen in RPMI-1640 containing 10% DMSO and stored in liquid nitrogen. All animals were handled according to the National Institutes of Health guidelines and studies were approved by the Animal Care and Use Committee of the NCI.

For apoptosis studies, 300,000 cells were plated in α-MEM media containing 20% FBS in a 96-well format. The cells were treated with 15 μmol/L H89 for 30 minutes after which HA22 or LMB-11 was added. After 72 hours, cells were harvested, stained with antihuman-CD19-FITC, Annexin V-PE, and 7-AAD. The CD19-positive population was defined as ALL cells, of which the % living cells was determined as double negative for Annexin V-PE

and 7-AAD. Results were analyzed in Prism Graph and all values were normalized to only vehicle-treated sample.

## Results

**H89 enhanced cytotoxic activity of CD22-targeting RITs *in vitro***

Figure 1 shows that H89 greatly increased the activity of CD22-targeting RITs. The $IC_{50}$ of LMB-11 on KOPN-8 was enhanced nine-fold from 1.1 to 0.13 ng/mL by 10 μmol/L H89 (Fig. 1A). Cytotoxic activity of HA22 was shifted from 0.08 to 0.03 ng/mL (Fig. 1B). To test if the enhancing effect of CD22-RITs was depending on a catalytically active PE, we combined H89 with the inactive LMB-11-E553D mutant LMB-31 (34). Neither LMB-31 alone nor the combination with H89 showed cytotoxic activity (Fig. 1C). To show that the H89 effect was target dependent, we tested the mesothelin-targeting RIT RG7787. RG7787 had no cytotoxic effect against mesothelin-negative KOPN-8 and there was no increase in RG7787 cytotoxicity by the addition of H89 (Fig. 1D). We also examined the effect of H89 on cycloheximide, an agent that inhibits protein synthesis by a different mechanism than RITs and found no enhancement (Fig. 1E). H89 itself had minimal inhibitory effects on KOPN-8 growth rate at 2.5 or 5 μmol/L. At 10 μmol/L H89, KOPN-8 cell growth was inhibited 20% (data not shown). These data together indicated that H89 specifically enhanced the activity of CD22-targeted RITs against KOPN-8 cells. We then examined the effects of H89 on four other ALL cell lines, Hal-01, NALM-6, SEM, and REH. As shown in Fig. 1F, H89 enhanced LMB-11 activity by 3- to 10-fold. The enhancement of H89 on different cell types ($IC_{50}$) is summarized in Supplementary Table S1.

**H89 increased inhibition of protein synthesis, but did not change the rate of internalization or furin-cleavage**

To investigate the mechanism of cytotoxicity enhancement by H89, we first evaluated the internalization rate of Alexa647-labeled LMB-11. Figure 2A shows that the amount of internalized LMB-11-Alexa647 over time was the same for H89 or vehicle treated KOPN-8. After RIT internalization, the protease furin cleaves PE between residues 279 and 280, which liberates the catalytically active 35 kDa PE fragment from the antibody moiety (19). Because LMB-11 was de-immunized by removing B-cell epitopes (17), antibodies against PE recognize this immunotoxin and its cleaved fragment very weakly, and thus cannot be used to detect the cleaved product of LMB-11. However, our antibodies bind strongly to the wild-type HA22. Because the rate of internalization was similar for Alexa647-labeled HA22 or LMB-11 and enhancement of their cytotoxic activity by H89 was comparable, we measured changes in the rate of furin-cleavage for HA22. As shown in Fig. 2B, the cleaved 35 kDa fragment became detectable after 30 minutes and increased up to 2 hours. There was no difference between control and H89-treated samples in the rate of furin cleavage.

We next evaluated if H89 enhanced the ability of RIT to arrest protein synthesis in KOPN-8 cells. We measured the rate of $^{3}$H-Leucine incorporation after cells were treated with LMB-11 with or without H89 and found that arrest of protein synthesis was enhanced 10-fold by H89 (Fig. 2C); H89 itself did not inhibit protein synthesis in KOPN-8 (Fig. 2C).

**H89 induced earlier ADP ribosylation and PARP cleavage**

Because protein synthesis arrest by RIT is a result of ADP ribosylation of eEF2, we determined if the increased arrest of

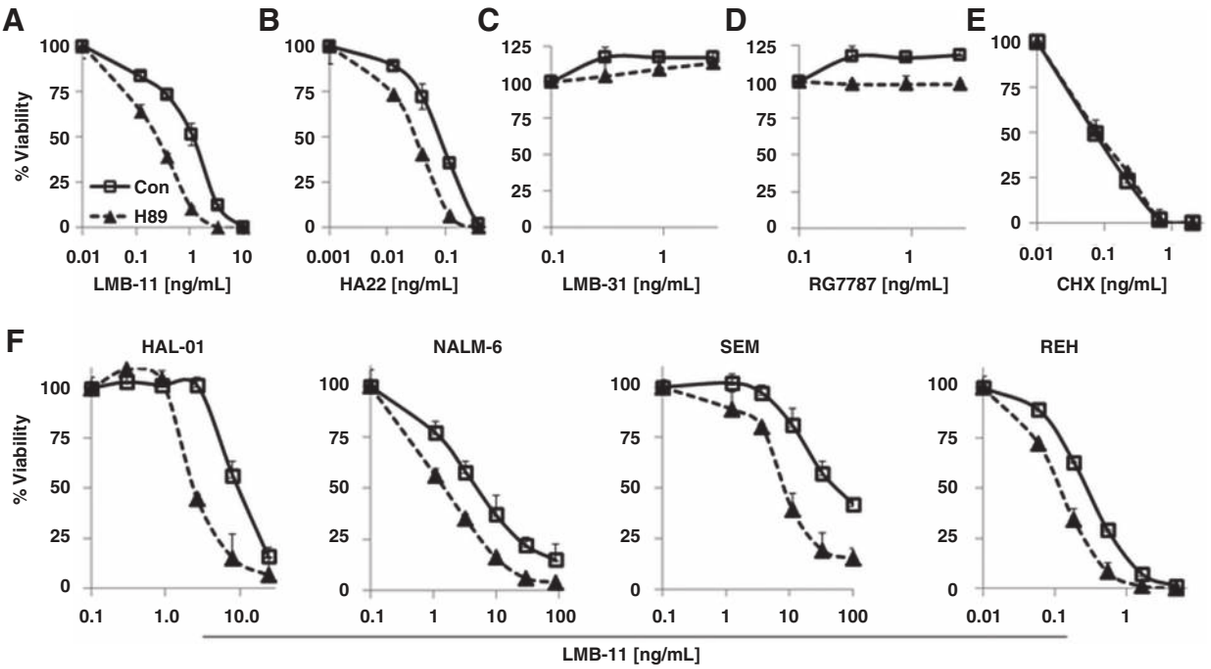


**Figure 1.**
H89 specifically enhanced CD22-targeting RITs. A and E, KOPN-8 cells were incubated with 10 μmol/L H89 or vehicle for 1 hour, then treated with LMB-11 (A), HA22 (B), LMB-31 (C), RG7787 (D) or cycloheximide (CHX; E) at indicated concentrations. For F, the ALL cell lines HAL-01, NALM-6, SEM, or REH were treated with 10 μmol/L H89 or vehicle for 1 hour after which LMB-11 was added at indicated concentrations. Cell viability was measured 72 hours later by WST8 assay, normalized to untreated control, and $IC_{50}$ determined using nonlinear regression.

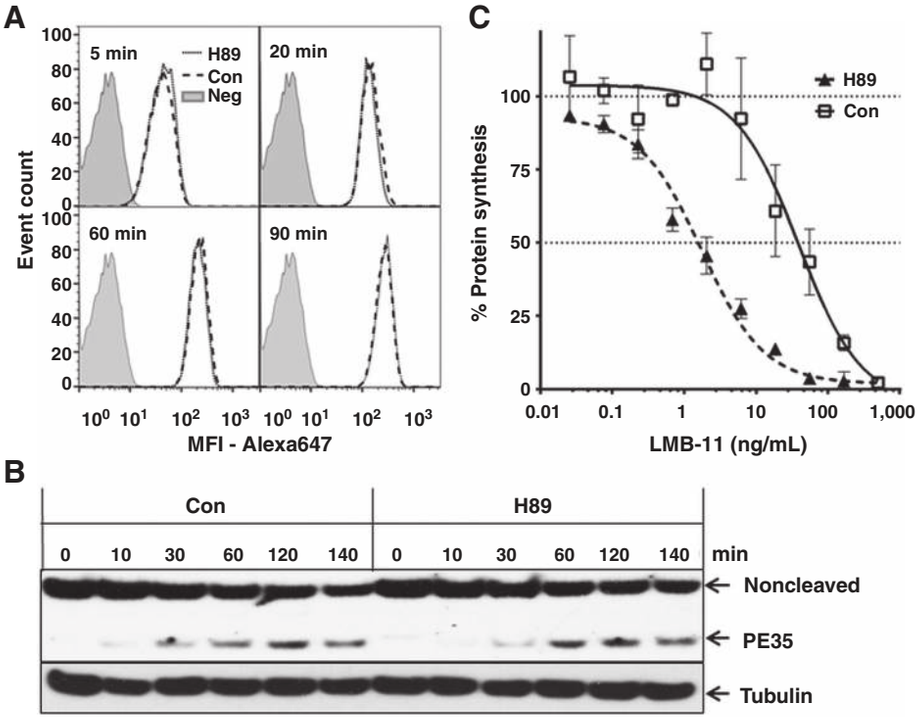


**Figure 2.**
H89 enhanced arrest of protein synthesis, but not RIT uptake or furin cleavage. A, KOPN-8 cells were incubated with 10 μmol/L H89 or vehicle (Con) for 1 hour and then treated with LMB-11-Alexa647 for the indicated times at 37°C. Surface-bound LMB-11 molecules were stripped off before analysis by flow cytometry. Untreated and unstained cells defined background signal (neg). B, KOPN-8 cells were treated with 10 μmol/L H89 for 1 hour. HA22 was added at 1 μg/mL, incubated on ice for 30 minutes to allow for saturate binding, and then incubated at 37°C for the indicated times. Total cell lysates were analyzed with anti-PE by Western blot analysis. PE35 is the furin-cleaved catalytically active fragment of HA22. C, KOPN-8 cells were treated with 10 μmol/L H89 or vehicle (Con) for 1 hour after which LMB-11 was added. Rate of protein synthesis was determined 16 hours later by incorporation of $^{3}$H-leucine. Values represent averages of three reads and are background subtracted absolute counts per minute (CPM).

protein synthesis by H89 correlated with an increase in the level of eEF2-ADP-ribose. KOPN-8 cells were incubated with LMB-11 and 10 μmol/L H89 or vehicle for up to 10 hours. Cell lysates were prepared at various times and the cell extract treated with biotinylated NAD and RIT to ADP-ribosylate unmodified eEF2. In untreated cells, eEF2 is not ADP ribosylated, so RIT added biotin-ADP-ribose maximally on eEF2 in the cell-free reaction. Figure 3A shows that in cells treated with LMB-11 alone, the level of ADP-eEF2 fell slowly and even after 10 hours of treatment, 20% of the eEF2 could still be modified with biotin-ADP-ribose. In cells treated with H89 and LMB-11, there was a very rapid fall in the amount of eEF2 that could be ADP ribosylated. The signal for biotin-ADP-ribose was undetectable from 8 hours with the combination (Fig. 3A). This increase in ADP ribosylation corresponded to the increased arrest of protein synthesis (Fig. 2C). To assess whether the H89 effect was observed with another cell line, we examined LMB-11-treated SEM cells and found that H89 similarly increased ADP ribosylation of eEF2 (Supplementary Fig. S1).

As a result of RIT-induced arrest of protein synthesis, MCL1 levels fall, which triggers induction of intrinsic apoptosis (35). As shown in Fig. 3A, KOPN-8 cells treated with LMB-11 alone showed a reduction of MCL1 levels after 10 hours. With the addition of H89, the level of MCL1 fell very rapidly below the detection limit after only 4 hours. Accordingly, cleaved PARP was detected earlier with combination treatment (Fig. 3A). Because high doses of LMB-11 (200 ng/mL) with H89 eliminated MCL1 levels, we studied combination treatment using a lower concentration of LMB-11 (5 ng/mL). Each agent alone reduced MCL1 by approximately 50% after 24 hours, and when combined, MCL1 was no longer detectable (Supplementary Fig. S2A). Levels of other apoptosis regulating proteins such as Bcl2, Bax, and Bak did not change within 24 hours.

The experiments described above measure early and intermediate events in RIT action, but do not measure cell death. To ensure that the changes in biochemical events studied ultimately resulted in an earlier and higher rate of apoptosis, we quantified cell death after 24 or 48 hours of treatment using flow cytometry. Figure 3B shows that 3 or 6 ng/mL LMB-11 alone had little effect on KOPN-8 after 24 hours of treatment. But at 48 hours there was 50% death with 3 ng/mL and 75% with 6 ng/mL. When 10 μmol/L H89 was added to LMB-11, significant cell death was observed after 24 hours and most cells were dead at 48 hours. H89 itself did not induce any cell death up to 48 hours.

### PKA-specific inhibitor PKI and cAMP-regulators did not change LMB-11 activity

We next investigated which of the H89 targets was responsible for the observed enhancing effects. H89 has been developed as PKA inhibitor, but it also inhibits other kinases (36). We tested if other PKA regulators would modulate RIT activity. To our surprise, the addition of a more specific PKA inhibitor, PKI, did not enhance LMB-11 (Fig. 4A). Furthermore, the PKA activating molecules dibutyryl-cAMP (Fig. 4B), 8-Br-cAMP, or Forskolin (Supplementary Fig. S3A and S3B) did not decrease the cytotoxic activity of LMB- 11. These data indicate that inhibition of PKA is not likely responsible for the H89-associated increase in LMB-11 activity.

### H89 inhibited S6 kinase 1

To investigate which kinases besides PKA were inhibited by H89, we screened a panel of 359 protein kinases for H89 inhibitory activity. Supplementary Table S2 shows that H89 inhibited 21 kinases by 90% or more. To examine the relevance of these kinases, we measured RNA levels of the 21 kinases in an internal

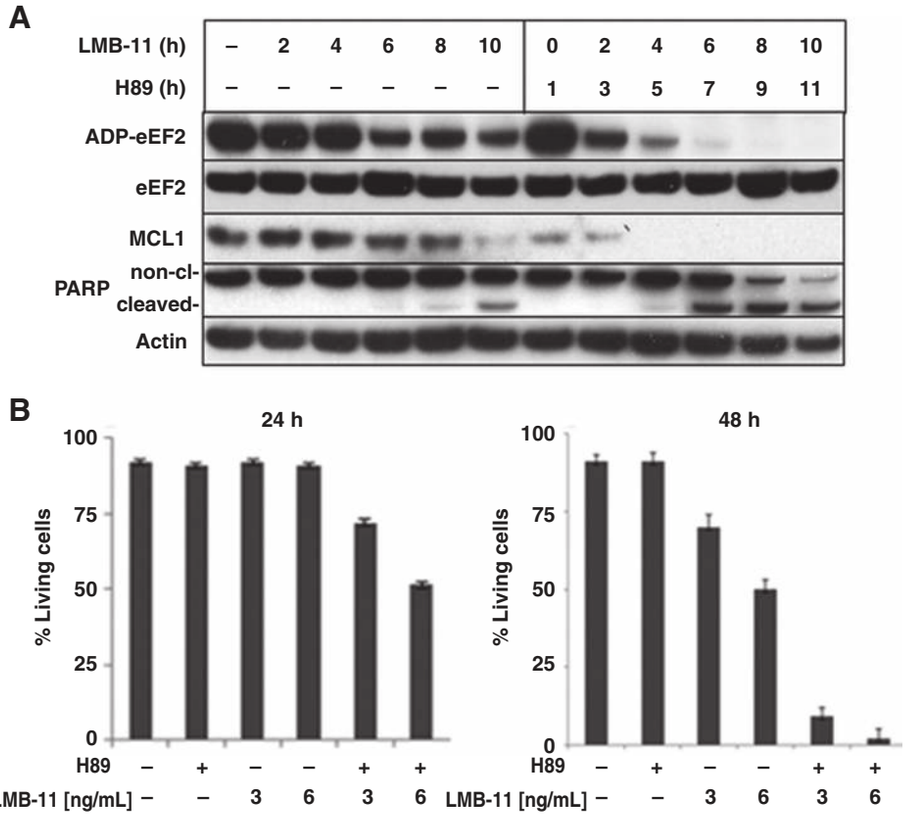


**Figure 3.**
H89 increased ADP-ribosylation of eEF2 and rate of apoptosis. A, KOPN-8 cells were treated with 10 μmol/L H89 for 1 hour, then, 200 ng/mL of LMB-11 was added for the indicated times before cell lysis, followed by Western blot analysis for Mcl-1, cleaved PARP, and actin. Not yet modified eEF2 in the cell lysates was labeled in a cell-free reaction with biotinylated ADP by LMB-11 as described in methods. B, KOPN-8 cells were treated with 10 μmol/L H89 or vehicle for 1 hour, then left untreated or treated with the indicated concentrations of LMB-11 for 24 (left) or 48 hours (right), respectively. Cells were then stained with Annexin V-PE and 7-AAD. Living cells were defined as double negative and blotted as percentage of all cells. Standard errors of mean were generated from three independent experiments.

RNA deep sequencing dataset. The RPKM values for the 21 kinases from the ALL cells KOPN-8, REH, NALM-6, SEM, and HAL-01 were averaged. We defined the threshold for relevant mRNA levels to be greater than an RPKM of 10 (31). Fourteen of the kinases that were inhibited more than 90% by H89 had an average RPKM above 10. We tested these 14 kinases for their RIT-enhancing activity using pharmacological inhibitors. Two of the 14 kinases partially recapitulated the H89 induced LMB-11 enhancement. p70S6-kinase (S6K1) inhibitor PF4708671 enhanced LMB-11 activity up to two-fold in a concentration dependent manner and the ROCK2 kinase inhibitor, Stemolecule, also produced a two-fold enhancement of LMB-11 activity (Supplementary Fig. S3C and S3D). However, neither of the kinase inhibitors alone or in combination (data not shown) replicated the strong enhancement of LMB-11 by H89 against KOPN-8 cells.

We analyzed the phospho-protein levels of relevant targets by Western blot to determine biochemical changes under H89 treatment. As shown in Fig. 4C, phospho-CREB and phospho-ATF1, two targets of PKA, underwent only minor changes in cells treated with H89. Vehicle-treated cells showed an elevation of the level of S6K1-(T389)-phosphorylation after 15 minutes, which increased further up to 2 hours. With the addition of H89, the p-S6K1-(T389) elevation was largely reduced whereas total S6K1 remained unaltered. The phosphorylation levels of S6K1 targets rpS6 (ribosomal protein S6) and p-GSK3β fell rapidly within 5 minutes and stayed low (p-GSK3β) or undetectable (p-rpS6) for 120 minutes. The total level of the antiapoptotic protein MCL1 was decreased 5 minutes after the addition of H89 and remained low for the 2 hour treatment period. In accordance with our inhibitor studies, phosphorylation of PKA targets changed very little which supports our earlier conclusion that PKA inhibition is not responsible for the enhancement by H89.

### H89 enhanced cytotoxicity of RITs targeting mesothelin

To determine if the robust enhancement of cytotoxicity was specific to CD22-targeting RITs, we studied H89 in combination with anti-mesothelin RITs that target epithelial cancers. As shown in Fig. 5A, SS1P (28, 29), which is similar in structure to HA22, has an $IC_{50}$ on KB31 cells of 11 ng/mL, which is lowered nine-fold to 1.3 ng/mL by 10 μmol/L H89 and 38-fold to 0.3 ng/mL by 15 μmol/L H89. Similarly, the $IC_{50}$ of RG7787, an $F_{ab}$ containing mesothelin-targeting RIT the construct of which resembles LMB-11 (31), was reduced from 12 to 3 and 1.2 ng/mL by 10 or 15 μmol/L H89, respectively (Fig. 5B).

Because WST8 assays measure mainly cell growth inhibition, we confirmed improved cell killing by H89 using light microscopy. KB31 cells treated with RG7787 at 20 ng/mL or H89 at 15 μmol/L alone were not killed in 3 days. But when H89 and RG7787 at these same concentrations were combined, cells died within 3 days (Fig. 5C). Induction of cell death after treatment with the combination of H89 and RG7787 was also confirmed by flow cytometry after staining with 7-AAD and Annexin V. We also analyzed biochemical changes for the combination treatment against KB31 to confirm the mechanism of action. As seen in KOPN-8, MCL1 was only marginally reduced after 24 hours of treatment with either H89 or RIT alone, but was abolished when the two were combined (Supplementary Fig. S2B). The

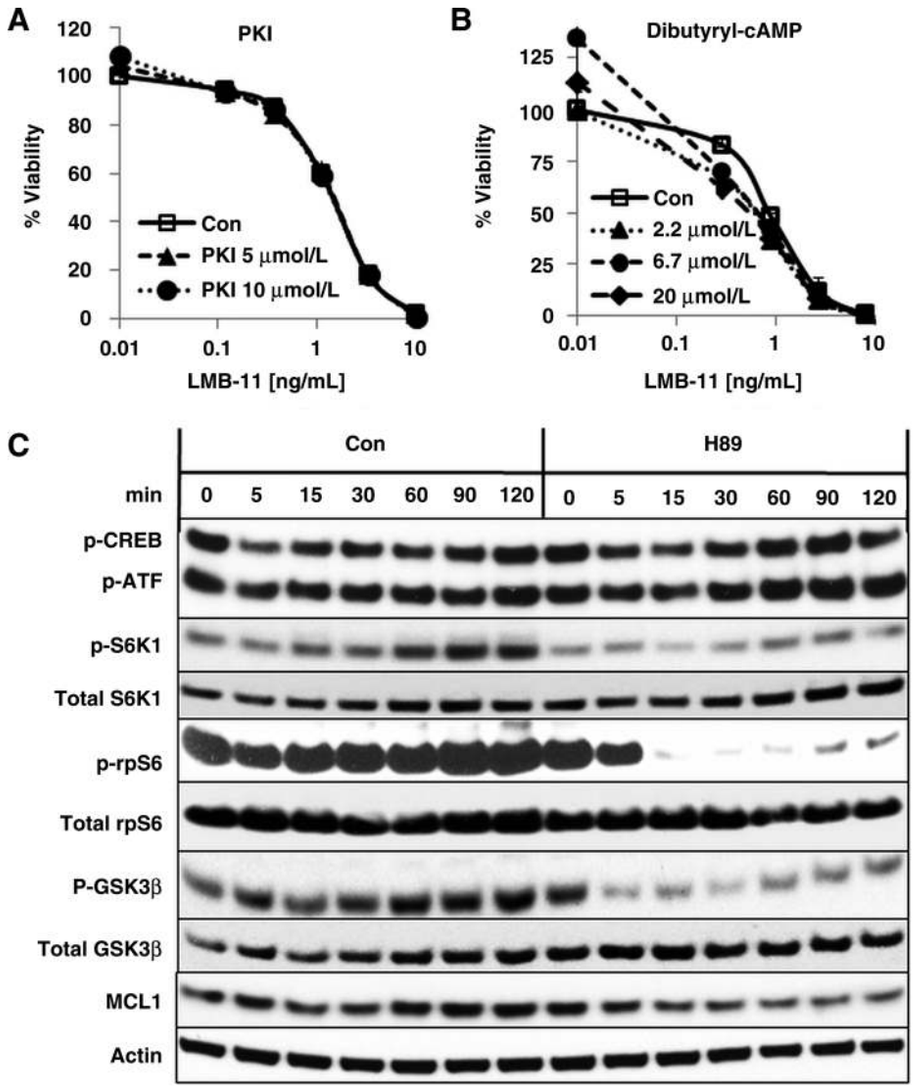


**Figure 4.**
PKA regulators did not affect LMB-11 activity; H89 inhibited S6K1 activity. A and B, KOPN-8 cells were treated with indicated concentrations of PKI (A) or Dibutyryl-cAMP (B) for 1 hour and then with indicated concentrations of LMB-11 for 72 hours. Cell viability was measured by WST8 assays. C, KOPN-8 cells were treated with 10 μmol/L H89 or vehicle (Con) for the indicated times. Total cell lysates were analyzed by Western blot analysis for anti-phospho-S6-Kinase 1 [p-S6K1(T389)], anti-total S6K1, anti-p-CREB(S133)/p-ATF-1, anti-p-ribosomal protein S6 [p-rpS6(S240/244)], anti-total rpS6, p-GSK3β(S9), anti-total GSK3β, anti-MCL1 and actin.

combination of RIT and H89 was also more potent in inducing PARP cleavage than either drug alone.

**H89 enhanced RIT on patient-derived ALL**

We tested H89 on patient-derived ALL samples to determine if the effects of H89 might be clinically relevant. Because these ALL cells had been propagated through murine xenografts, we used flow cytometry to determine the living cells of the human ALL population for each sample. We treated four patient-derived samples *in vitro* with immunotoxins HA22 or LMB-11 in combination with H89. H89 greatly enhanced RIT-activity in all four samples (Fig. 6A and B). H89 by itself did not kill patient samples 1, 2, and 4 (all data in Fig. 6 were normalized to only vehicle-treated cells), but significantly increased both HA22 and LMB-11 killing 3- to 10-fold. Cells from patient 3 were resistant to both HA22 and LMB-11. When H89 was added, 40% of the cells died within 3 days because of the inhibitor alone. The combination of H89 with either HA22 or LMB-11 resulted in a dose-dependent killing of most of the prior RIT-resistant cells.

## Discussion

We show that the protein kinase inhibitor H89 enhances the cytotoxic activity of CD22-targeting immunotoxins LMB-11 and HA22 on ALL cell lines and the cytotoxic activity of mesothelin-targeting RITs SS1P and RG7787 on KB31 cells. In addition, H89 enhances RIT-induced cell killing on patient-derived ALL cells, which supports the clinical relevance of these findings. We demonstrated the H89 effect to be dependent on a catalytically active PE and specific for PE-induced arrest of protein synthesis on eEF2. Cell death produced by cycloheximide, a protein synthesis inhibitor that has a different mechanism of action, was not enhanced by H89. H89 activity was partially recapitulated by inhibition of S6K1, resulting in a fall in MCL1. This S6K1 induced reduction of MCL1 worked together with the fall in MCL1 because of arrest of protein synthesis by RIT, ultimately increasing apoptosis.

H89 was developed as a competitive inhibitor for ATP binding to PKA. It is now known that H89 also inhibits other kinases such as ROCK2, S6K1, MSK1/2, or RSK (36–38). Our *in vitro* kinase screen confirmed that H89 not only inhibited these kinases, but

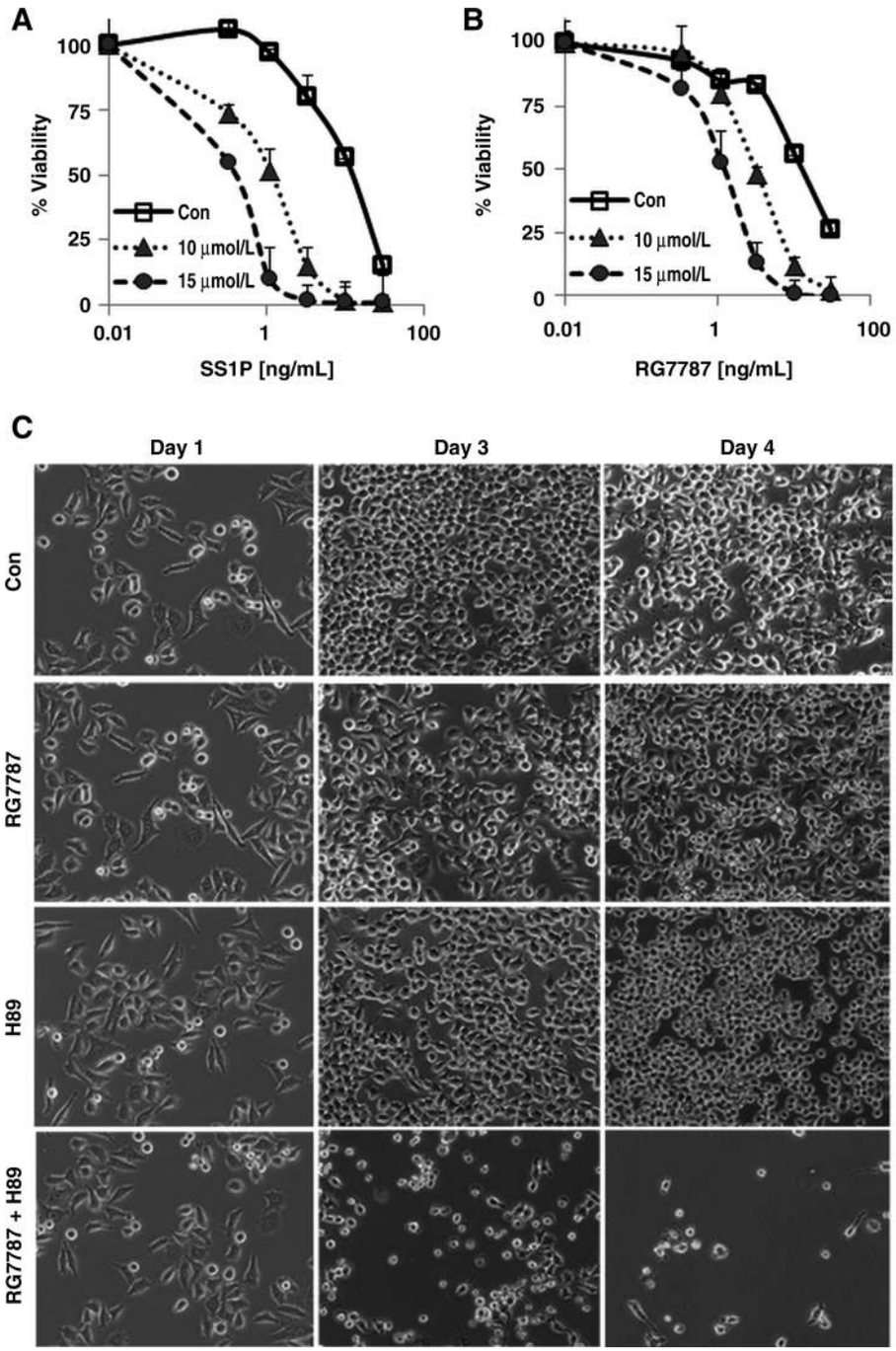


**Figure 5.**
H89 enhanced anti-mesothelin RIT-induced cytotoxicity against KB31 cells. A and B, KB31 cells were treated with 10 μmol/L H89 for 1 hour. Then, indicated concentrations of SS1P (A) or RG7787 (B) were added. Cell viability was determined by WST8 assay. C, KB31 cells were plated on day 0, grown overnight in six-well plates and on day 1 simultaneously treated with the combination of 20 ng/mL RG7787 and 15 μmol/L H89 or vehicle. Images were taken at the day of treatment (Day 1) and on days 3 and 4.

also other AGC kinase subfamily members (39) including AKT, PKC, PKN, PKG, LATS, PRKX, and NDR2, as well as kinases unrelated to the AGC subfamily including FAK/PTK2 and ARK5/NUAK1.

Because we found the S6K1 inhibitor PF4708671 was a less potent RIT activator than H89, we tested the biochemical changes produced when it was combined with LMB-11. As expected from the S6K1 inhibition, the combination of PF4708671 with LMB-11 resulted in a rapid fall in MCL1 (Supplementary Fig. S4) similar to the effects of H89. But PF4708671 only slightly enhanced the ADP-ribosylation of eEF2 showing a striking difference between the two S6K1 inhibiting molecules. We interpret this as a possible explanation for the stronger RIT enhancement with H89 than with PF4708671. That none of the tested inhibitors for GSK3β, S6K1, or ROCK2 alone or in combination were able to mimic the enhancement of LMB-11 by H89 suggest that the strong RIT enhancing effects by H89 are based on the inhibition of more than one kinase.

The mechanism by which H89 enhances RIT activity appears to involve at least two major events in RIT-induced cell death,

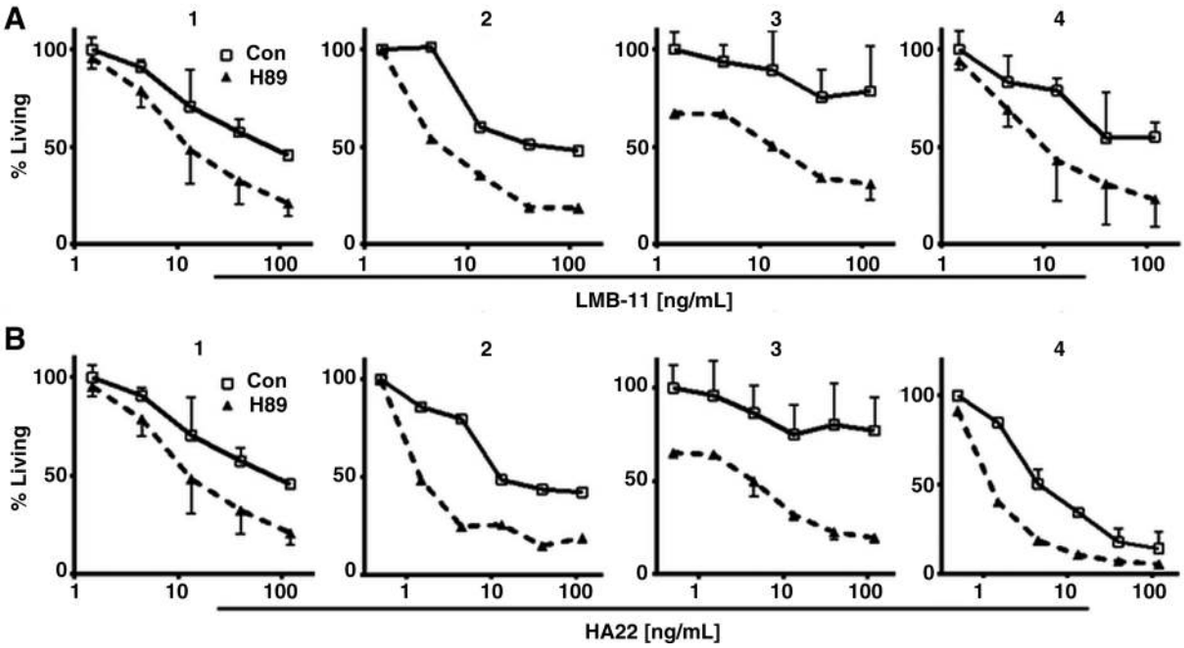


**Figure 6.**
H89 enhanced activity of RIT on patient-derived ALL cells. Four patient-derived ALL samples were propagated in mice, extracted from murine spleen, and viably frozen. Thawed samples were treated with 15 μmol/L H89 for 1 hour. Then, LMB-11 (A) or HA22 (B) was added at indicated concentrations. After 72 hours, cells were stained with antihuman CD19-FITC, Annexin V-PE, and 7-AAD and analyzed by flow cytometry. ALL was defined as hu-CD19-positive. Percent living ALL cells were determined (negative for Annexin V-PE and 7-AAD) and normalized to RIT and H89 untreated control.

ADP ribosylation, and MCL1 degradation. H89 enhances ADP ribosylation of eEF2 by RITs, which leads to an enhanced arrest of protein synthesis (5, 12). That H89 did not enhance the catalytically inactive LMB-31 highlights the necessity of ADP ribosylation as a key event in the cell killing associated with the combination of H89 and LMB-11. Notably, H89 alone did not affect ADP ribosylation (Fig. 3A, time point 0). Together, these data suggest that an RIT-related process that precedes actual ADP ribosylation is altered by H89. This could be related to enhanced RIT transport to the endoplasmic reticulum or from the endoplasmic reticulum to the cytosol where eEF2 is located. Following protein synthesis inhibition because of the inactivation of eEF2, protein levels of the PEST-sequence containing MCL1 fall because of its rapid turnover (35).

Although H89 alone did not itself arrest protein synthesis, we observed that it had several effects of its own on cells. H89 reduced the phosphorylation of rpS6 (240/244) and abolished p-GSK3β (S9) at their respective S6K1 phosphorylation sites (40). This indicates that the activity of these well-established S6K1 targets is modulated by H89. The reduction of phosphorylation at Ser(9) of GSK3β results in an increase in its kinase activity. GSK3β phosphorylates MCL1 at Ser(159) within the PEST sequence which increases ubiquitination and degradation of MCL1 (41–43). We showed this synergistic decrease of MCL1 for both mesothelin- and CD22-targeting RITs. Of note, the levels of other apoptosis modulators like Bax, Bak, or Bcl2 were not changed; emphasizing the central role of MCL1 in the mechanism of H89 enhanced apoptosis induction by RITs.

MCL1 plays a pivotal role in protecting cells from apoptosis and this protein is overexpressed in many cancers (35, 44–46) including ALL subsets (47). Targeting MCL1 degradation represents an important pharmacological approach in cancer drug development (48). Therefore, the rapid fall of MCL1 with H89 treatment could explain the effective killing of cells from patient 3 that were otherwise RIT resistant.

H89 strongly enhanced immunotoxin activity against ALL cell lines and patient-derived cells as well as against an epithelial cancer cell line *in vitro*. These data strongly support further preclinical development of H89 for combination treatment with PE-based immunotoxins that target CD22 and mesothelin-expressing tumors.

## Disclosure of Potential Conflicts of Interest

A.S. Wayne reports receiving a commercial research grants from MedImmune; has received other commercial research support from Kite Pharma as a consultant; has received speakers bureau honoraria from Pfizer, MedImmune, and Kite Pharma; has ownership interest as co-investigator on patents assigned to the NIH; and is an advisory board member for Pfizer and Kite Pharma. I. Pastan has ownership interest as co-investigator on patents assigned to the NIH for investigational products. No potential conflicts of interest were disclosed by the other authors.

## Authors' Contributions

**Conception and design:** F. Müller, A.S. Wayne, I. Pastan
**Development of methodology:** X. Liu, F. Müller
**Acquisition of data (provided animals, acquired and managed patients, provided facilities, etc.):** X. Liu, F. Müller
**Analysis and interpretation of data (e.g., statistical analysis, biostatistics, computational analysis):** X. Liu, F. Müller, A.S. Wayne, I. Pastan
**Writing, review, and/or revision of the manuscript:** X. Liu, F. Müller, A.S. Wayne, I. Pastan
**Administrative, technical, or material support (i.e., reporting or organizing data, constructing databases):** I. Pastan
**Study supervision:** I. Pastan

## Acknowledgments

The authors thank Richard Beers for the cloning and expression of LMB-31.

## Grant Support

The work was supported in part by award number P30CA014089 from the National Cancer Institute, the Intramural Research Program of the NIH, National Cancer Institute, and the Center for Cancer Research, and by a Cooperative Research and Development Agreement (#1975) with MedImmune, LLC. F. Müller was supported in part by the German Research Foundation, award number MU 3619/1-1.

The costs of publication of this article were defrayed in part by the payment of page charges. This article must therefore be hereby marked *advertisement* in accordance with 18 U.S.C. Section 1734 solely to indicate this fact.

Received October 8, 2015; revised February 4, 2016; accepted February 4, 2016; published OnlineFirst March 3, 2016.

## References

1. Inaba H, Greaves M, Mullighan CG. Acute lymphoblastic leukaemia. Lancet 2013;381:1943–55.
2. Hunger SP, Lu X, Devidas M, Camitta BM, Gaynon PS, Winick NJ, et al. Improved survival for children and adolescents with acute lymphoblastic leukemia between 1990 and 2005: a report from the children's oncology group. J Clin Oncol 2012;30:1663–9.
3. Ko RH, Ji L, Barnette P, Bostrom B, Hutchinson R, Raetz E, et al. Outcome of patients treated for relapsed or refractory acute lymphoblastic leukemia: a Therapeutic Advances in Childhood Leukemia Consortium study. J Clin Oncol 2010;28:648–54.
4. Reis LAG, Smith MA, Gurney JG, et al. editors. Cancer incidence and survival among children and adolescents: United States SEER Program 1975–1995, National Cancer Institute, SEER Program. Childhood cancer mortality. NIH Publ. No. 99–4649. Bethesda, MD; 1999. p. 165–70.
5. Wayne AS, Fitzgerald DJ, Kreitman RJ, Pastan I. Immunotoxins for leukemia. Blood 2014;123:2470–7.
6. Maude SL, Frey N, Shaw PA, Aplenc R, Barrett DM, Bunin NJ, et al. Chimeric antigen receptor T cells for sustained remissions in leukemia. New Engl J Med 2014;371:1507–17.
7. Lee DW, Kochenderfer JN, Stetler-Stevenson M, Cui YK, Delbrook C, Feldman SA, et al. T cells expressing CD19 chimeric antigen receptors for acute lymphoblastic leukaemia in children and young adults: a phase 1 dose-escalation trial. Lancet 2015;385:517–28.
8. Topp MS, Gokbuget N, Zugmaier G, Degenhard E, Goebeler ME, Klinger M, et al. Long-term follow-up of hematologic relapse-free survival in a phase 2 study of blinatumomab in patients with MRD in B-lineage ALL. Blood 2012;120:5185–7.
9. Haso W, Lee DW, Shah NN, Stetler-Stevenson M, Yuan CM, Pastan IH, et al. Anti-CD22-chimeric antigen receptors targeting B-cell precursor acute lymphoblastic leukemia. Blood 2013;121:1165–74.
10. Li D, Poon KA, Yu SF, Dere R, Go M, Lau J, et al. DCDT2980S, an anti-CD22-monomethyl auristatin E antibody-drug conjugate, is a potential treatment for non-Hodgkin lymphoma. Mol Cancer Ther 2013;12:1255–65.
11. Wu AM, Senter PD. Arming antibodies: prospects and challenges for immunoconjugates. Nat Biotechnol 2005;23:1137–46.
12. Pastan I, Hassan R, Fitzgerald DJ, Kreitman RJ. Immunotoxin therapy of cancer. Nat Rev 2006;6:559–65.
13. Kreitman RJ, Stetler-Stevenson M, Margulies I, Noel P, Fitzgerald DJ, Wilson WH, et al. Phase II trial of recombinant immunotoxin RFB4 (dsFv)-PE38 (BL22) in patients with hairy cell leukemia. J Clin Oncol 2009;27:2983–90.
14. Shah NN, Stevenson MS, Yuan CM, Richards K, Delbrook C, Kreitman RJ, et al. Characterization of CD22 expression in acute lymphoblastic leukemia. Pediatr Blood Cancer 2015;62:964–9.
15. Kreitman RJ, Tallman MS, Robak T, Coutre S, Wilson WH, Stetler-Stevenson M, et al. Phase I trial of anti-CD22 recombinant immunotoxin moxetumomab pasudotox (CAT-8015 or HA22) in patients with hairy cell leukemia. J Clin Oncol 2012;30:1822–8.
16. Wayne AS, Shah NN, Bhojwani D, Silverman LB, Whitlock JA, Stetler-Stevenson M, et al. Pediatric phase 1 trial of moxetumomab pasudotox: activity in chemotherapy refractory acute lymphoblastic leukemia (ALL). Cancer Res 2014;74(19 Suppl). Abstract nr CT230.
17. Onda M, Beers R, Xiang L, Lee B, Weldon JE, Kreitman RJ, et al. Recombinant immunotoxin against B-cell malignancies with no immunogenicity in mice by removal of B-cell epitopes. Proc Natl Acad Sci USA 2011;108:5742–7.
18. Bera TK, Onda M, Kreitman RJ, Pastan I. An improved recombinant Fab-immunotoxin targeting CD22 expressing malignancies. Leuk Res 2014;38:1224–9.
19. Weldon JE, Pastan I. A guide to taming a toxin–recombinant immunotoxins constructed from *Pseudomonas* exotoxin A for the treatment of cancer. FEBS J 2011;278:4683–700.
20. Pasetto M, Antignani A, Ormanoglu P, Buehler E, Guha R, Pastan I, et al. Whole-genome RNAi screen highlights components of the endoplasmic reticulum/Golgi as a source of resistance to immunotoxin-mediated cytotoxicity. Proc Natl Acad Sci USA 2015;112:E1135–42.
21. Liu XF, FitzGerald DJ, Pastan I. The insulin receptor negatively regulates the action of Pseudomonas toxin-based immunotoxins and native Pseudomonas toxin. Cancer Res 2013;73:2281–8.
22. Liu XF, Xiang L, FitzGerald DJ, Pastan I. Antitumor effects of immunotoxins are enhanced by lowering HCK or treatment with SRC kinase inhibitors. Mol Cancer Ther 2014;13:82–9.
23. Chijiwa T, Mishima A, Hagiwara M, Sano M, Hayashi K, Inoue T, et al. Inhibition of forskolin-induced neurite outgrowth and protein phosphorylation by a newly synthesized selective inhibitor of cyclic AMP-dependent protein kinase, N-[2-(p-bromocinnamylamino)ethyl]-5-isoquinolinesulfonamide (H-89), of PC12D pheochromocytoma cells. J Biol Chem 1990;265:5267–72.
24. Davis MA, Hinerfeld D, Joseph S, Hui YH, Huang NH, Leszyk J, et al. Proteomic analysis of rat liver phosphoproteins after treatment with protein kinase inhibitor H89 (N-(2-[p-bromocinnamylamino-]ethyl)-5-isoquinolinesulfonamide).J Pharmacol Exp Ther 2006;318:589–95.
25. Marunaka Y, Niisato N. H89, an inhibitor of protein kinase A (PKA), stimulates Na+ transport by translocating an epithelial $Na^+$ channel (ENaC) in fetal rat alveolar type II epithelium. Biochem Pharmacol 2003;66:1083–9.
26. Reber LL, Daubeuf F, Nemska S, Frossard N. The AGC kinase inhibitor H89 attenuates airway inflammation in mouse models of asthma. PLoS One 2012;7:e49512.
27. Salvatore G, Beers R, Margulies I, Kreitman RJ, Pastan I. Improved cytotoxic activity toward cell lines and fresh leukemia cells of a mutant anti-CD22 immunotoxin obtained by antibody phage display. Clin Cancer Res 2002;8:995–1002.
28. Chowdhury PS, Pastan I. Improving antibody affinity by mimicking somatic hypermutation in vitro. Nat Biotechnol 1999;17:568–72.
29. Hassan R, Lerner MR, Benbrook D, Lightfoot SA, Brackett DJ, Wang QC, et al. Antitumor activity of SS(dsFv)PE38 and SS1(dsFv)PE38, recombinant antimesothelin immunotoxins against human gynecologic cancers grown in organotypic culture in vitro. Clin Cancer Res 2002;8:3520–6.
30. Pastan I, Beers R, Bera TK. Recombinant immunotoxins in the treatment of cancer. Methods Mol Biol 2004;248:503–18.
31. Hollevoet K, Mason-Osann E, Muller F, Pastan I. Methylation-associated partial down-regulation of mesothelin causes resistance to anti-mesothelin immunotoxins in a pancreatic cancer cell line. PLoS One 2015;10:e0122462.
32. Wei H, Xiang L, Wayne AS, Chertov O, FitzGerald DJ, Bera TK, et al. Immunotoxin resistance via reversible methylation of the DPH4 promoter is a unique survival strategy. Proc Natl Acad Sci USA 2012;109:6898–903.
33. Mason-Osann E, Hollevoet K, Niederfellner G, Pastan I. Quantification of recombinant immunotoxin delivery to solid tumors allows for direct comparison of in vivo and in vitro results. Sci Rep 2015;5:10832.

34. Jorgensen R, Wang Y, Visschedyk D, Merrill AR. The nature and character of the transition state for the ADP-ribosyltransferase reaction. EMBO Rep 2008;9:802–9.
35. Du X, Youle RJ, FitzGerald DJ, Pastan I. *Pseudomonas* exotoxin A-mediated apoptosis is Bak dependent and preceded by the degradation of Mcl-1. Mol Cell Biol 2010;30:3444–52.
36. Murray AJ.Pharmacological PKA inhibition: all may not be what it seems. Sci Signal 2008;1:re4.
37. Hidaka H, Inagaki M, Kawamoto S, Sasaki Y. Isoquinolinesulfonamides, novel and potent inhibitors of cyclic nucleotide dependent protein kinase and protein kinase C. Biochemistry 1984;23:5036–41.
38. Lochner A, Moolman JA. The many faces of H89: a review. Cardiovasc Drug Rev 2006;24:261–74.
39. Pearce LR, Komander D, Alessi DR. The nuts and bolts of AGC protein kinases. Nat Rev Mol Cell Biol 2010;11:9–22.
40. Zhang HH, Lipovsky AI, Dibble CC, Sahin M, Manning BD. S6K1 regulates GSK3 under conditions of mTOR-dependent feedback inhibition of Akt. Mol Cell 2006;24:185–97.
41. Ding Q, He X, Hsu JM, Xia W, Chen CT, Li LY, et al. Degradation of Mcl-1 by beta-TrCP mediates glycogen synthase kinase 3-induced tumor suppression and chemosensitization. Mol Cell Biol 2007;27:4006–17.
42. Maurer U, Charvet C, Wagman AS, Dejardin E, Green DR. Glycogen synthase kinase-3 regulates mitochondrial outer membrane permeabilization and apoptosis by destabilization of MCL-1. Mol Cell 2006; 21:749–60.
43. Zhong Q, Gao W, Du F, Wang X. Mule/ARF-BP1, a BH3-only E3 ubiquitin ligase, catalyzes the polyubiquitination of Mcl-1 and regulates apoptosis. Cell 2005;121:1085–95.
44. Mitchell C, Yacoub A, Hossein H, Martin AP, Bareford MD, Eulitt P, et al. Inhibition of MCL-1 in breast cancer cells promotes cell death in vitro and in vivo. Cancer Biol Ther 2010;10:903–17.
45. Song L, Coppola D, Livingston S, Cress D, Haura EB. Mcl-1 regulates survival and sensitivity to diverse apoptotic stimuli in human non-small cell lung cancer cells. Cancer Biol Ther 2005;4:267–76.
46. Inuzuka H, Fukushima H, Shaik S, Liu P, Lau AW, Wei W. Mcl-1 ubiquitination and destruction. Oncotarget 2011;2:239–44.
47. Koss B, Morrison J, Perciavalle RM, Singh H, Rehg JE, Williams RT, et al. Requirement for antiapoptotic MCL-1 in the survival of BCR-ABL B-lineage acute lymphoblastic leukemia. Blood 2013;122:1587–98.
48. Quinn BA, Dash R, Azab B, Sarkar S, Das SK, Kumar S, et al. Targeting Mcl-1 for the therapy of cancer. Expert Opin Investig Drugs 2011; 20:1397–411.